Supporting information for

Controlled O_2 reduction at a mixed-valent (II,I) Cu_2S core.

Jordan Mangue,[a] Clément Gondre,[a] Jacques Pécaut,[b] Carole Duboc,[c] Stéphane Ménage[a] and Stéphane Torelli*[a]

[a] Univ. Grenoble Alpes, CNRS, CEA, IRIG, Laboratoire de Chimie et Biologie des Métaux, 17 rue des Martyrs, 38054 Grenoble Cedex 9, France.

[b] Univ. Grenoble Alpes, CEA, CNRS, IRIG, SYMMES, UMR 5819 Equipe Chimie Interface Biologie pour l'Environnement, la Santé et la Toxicologie, 38054 Grenoble Cedex 9, France

[c] Univ. Grenoble Alpes, Département de Chimie Moléculaire, 301 rue de la chimie, 38054 Grenoble Cedex 9, France.

Correspondence should be addressed to stephane.torelli@cea.fr

Table of Contents

Figure S6. Kinetic profiles (Abs_{max}^{750nm}) for the catalytic ORR by **1** with $LutHBF_4$ and Me_8Fc (80 and 100 molar eq.) in air-saturated MeCN.

Figure S7. Kinetic profiles (Abs_{max}^{778nm}) for the catalytic ORR by **1** with $LutHBF_4$ and $Me_{10}Fc$ (10, 20, 40 and 60 molar eq.) in air-saturated MeCN.

Figure S8. Kinetic profiles (Abs_{max}^{778nm}) for the catalytic ORR by **1** with $LutHBF_4$ and $Me_{10}Fc$ (80 and 100 molar eq.) in air-saturated MeCN.

Figure S9. H_2O_2 calibration curve using the TiO-tpyp reagent and corresponding UV-vis traces

Figure S10. Control experiments.

Figure S11. Plot of the *pseudo*-first-order rate constants (k_{obs}) versus [$Me_{8\text{-}10}Fc$] for the ORR catalysed by **1** in the presence of 400 molar eq. $LutHBF_4$ in air-saturated MeCN at 298 K.

Figure S12. Me_8Fc^+ accumulation (by monitoring the absorbance at 750 nm) upon successive runs under H_2O_2 production conditions; [**1**] = 0.05 mM, **1** /Me_8Fc/$LutHBF_4$ at 1/10/400, air-saturated MeCN, 298 K.

Figure S13. Changes in the UV-vis/NIR spectrum of **1** (0.75 mM) in the presence of proton and electron sources under inert atmosphere.

Figure S14. Changes in the X-band (9.39 GHz) EPR spectrum of **1** upon subsequent reaction with $LutHBF_4$ (400 molar eq.) and Me_8Fc (10 molar eq.) or a mixture of both reagents in MeCN under inert atmosphere at 42 K.

Figure S15. Electrospray ionization mass spectrum of *in situ* generated $\mathbf{1_{red}}^{H}$ from the reaction of **1** with $LutHBF_4$ and Me_8Fc in MeCN.

Figure S16. X-ray crystal structure of $\mathbf{1_{ox}}$.

Figure S17. UV-vis/NIR spectra of **1** before and after exposure to air ($\mathbf{1_{ox}}$) in MeCN at 298 K.

Figure S18. Changes in the X-band (9.39 GHz) EPR spectrum of **1** before and after exposure to air ($\mathbf{1_{ox}}$) in MeCN at 42 K.

Figure S19. Electrospray ionization mass spectrum of $\mathbf{1_{ox}}$ generated from air oxidation of a MeCN solution of **1**.

Figure S20. Kinetic profiles (Abs_{max}^{750nm}) resulting from the reaction of $\mathbf{1_{ox}}$ with an air-saturated MeCN mixture of Me_8Fc and $LutHBF_4$ (1/10/400).

Figure S21. Changes in the UV-vis spectrum of $\mathbf{1_{ox}}$ (0.5 mM) consecutive to the addition of $LutHBF_4$, Me_8Fc or a combination under inert atmosphere in MeCN at 298 K.

Figure S22. Possible routes for the formation of $\mathbf{1_{red}^{H}}$ starting from **1**.

Figure S23. Electrospray ionization mass spectrum of the final reaction mixture obtained upon air exposure of a combination of **1** + $LutHBF_4$ and Me_8Fc in MeCN.

Table S1. Calculated maximum absorbance values for the tested experimental conditions.[(a)]

Table S2. k_{obs} (s^{-1}) values obtained from mono- or bi-exponential fits of the kinetics traces corresponding to the accumulation of ferrocenium derivatives at the appropriate λ_{max}.

Table S3. Crystal data and structure refinement for $\mathbf{1_{ox}}$.

Table S4. Bond length [Å] and angles [deg] for $\mathbf{1_{ox}}$.

Experimental section

General. ***All chemicals*** are from Acros Organics, Merck, or Lancaster. Acroseal® purity solvents were used for air-sensitive experiments. Complex **1** was prepared according to our reported procedure.[1] $LutHBF_4$, Me_8Fc, Me_2Fc^+, Me_8Fc^+ and $Me_{10}Fc^+$ were prepared according to reported procedures.[2] Air-sensitive materials were manipulated in an Argon flushed glove box (O_2 and H_2O < 2 ppm). **Mass spectrometry spectra** were recorded with a Bruker Daltonics Esquire 3000 Plus (ESI-MS) device. **X-ray crystallography** data were acquired at 150 K using an Oxford-diffraction XCalibur S diffractometer with graphite monochromated MoKα radiation (λ = 0.71073 Å). Molecular structure was solved by direct methods and refined on F^2 by full matrix least squares techniques using SHELX TL package. All non-hydrogen atoms were refined anisotropically, and hydrogen atoms were placed in ideal positions and refined as riding atoms with individual isotropic displacement parameters. **X-band EPR** spectra were obtained on a Bruker EMX spectrometer equipped with an Oxford ESR 910 cryostat for low temperature studies. The microwave frequency was calibrated with a frequency counter and the magnetic field with an NMR gaussmeter. Spectra were analysed with the WIN-EPR software. When required, spin quantification was done using a Cu^{II} standard as reference ($[Cu^{II}]$ = 0.95 mM) and the following equation:

$$C(u) = \frac{In(u) * 0.00095}{In(st)}$$

Where:

C*(u)* is the S=1/2 concentration to be determined in the sample,

I*n(u)* is the normalized integral (DI/N) of the sample,

I*n(st)* is the normalized integral (DI/N) of the Cu^{II} standard.

UV-vis/NIR spectra were recorded on a Perkin Elmer Lambda 1050 Spectrophotometer operating at room temperature equipped with appropriate optic fibres and connected to a glovebox. Spectral adjustments were performed using the Origin software. **Kinetics** were recorded with a Lambda 465 (PerkinElmer) diode array spectrophotometer and **H_2O_2 concentrations** were determined according to the procedure described below using a Shimadzu 1800 device.

X-ray quality crystals of 1_{ox} were obtained as follow:

A MeCN solution of 1 was exposed to air, leading to a colour change from purple to dark green. The resulting solution was evaporated to dryness. X-ray quality crystals were grown for diffusion of Et_2O into a CH_2Cl_2 solution of **1_{ox}**. The CCDC deposition number for **1_{ox}** is 2014256.

Catalytic H_2O_2 production, detection and quantification.

The formation of Fc^+, Me_2Fc^+, Me_8Fc^+ or $Me_{10}Fc^+$ in the presence of **1** or $[Cu(Tol)_2](OTf)$ (OTf = trifluoromethanesulfonate anion and Tol = toluene) and *2,6*-lutidinium tetrafluoroborate ($LutHBF_4$) was monitored in air-saturated MeCN at 298 K by visible absorption spectroscopy. In a typical experiment (1/40/400), an air-saturated solution of $LutHBF_4$ (25 µL, 2.0 M, 50 µmol, 400 molar eq.) was added to an air-saturated solution of Me_8Fc (2.225 mL, 2.24 mM, 4.98 µmol, 40 molar eq.) in a septum-sealed quartz cuvette (1 cm). An Ar-saturated solution of **1** (250 µL, 0.5mM, 0.125 µmol, 1 molar eq.) was then added. Kinetics traces at λ_{max}^{Fc+} (614 nm, ε = 410 M^{-1} cm^{-1}), λ_{max}^{Me2Fc+} (650 nm, ε = 290 M^{-1} cm^{-1}), λ_{max}^{Me8Fc+} (750 nm, ε = 390 M^{-1} cm^{-1}) and $\lambda_{max}^{Me10Fc+}$ (779 nm, ε = 495 M^{-1} cm^{-1}) (Fig. S1) were monitored using a Lambda 465 (PerkinElmer) diode array spectrophotometer (Δt = 0.5 s or 1 s). Control experiments (Fig. S10) were performed in an identical manner by adding $[Cu(Tol)_2](OTf)$ in MeCN, (250 µL, 0.5 mM, 0.125 µmol), MeCN (250 µL) or H_2O_2 (250 µL, 0.5 M, 125 µmol, 100 molar eq.) instead of **1**. All the experiments were triplicated, yielding highly reproducible data (96% identity). The amount of hydrogen peroxide produced was determined by spectroscopic titration with an acidic solution of $TiO(tpypH_4)^{4+}$ complex (TiO-tpyp reagent).[3] The TiO-tpyp reagent (~4.5. 10^{-5} M) was prepared by dissolving 3.45 mg of the [TiO(tpyp)] complex (≥90%, from TCI) in 100 mL of 0.05 M $HCl_{(aq)}$ and stored at 277 K. A small portion (15 µL) of each sample solution (collected after observing stable absorbance values along

time) was added to a mixture of TiO-tpyp reagent (250 µL), 4.8 M perchloric acid (250 µL) and water (235 µL). The resulting solution was stirred for 5 min at 298 K. After dilution to 2.5 mL with distilled water, the solution was transferred in a quartz UV-vis cell (1 mm) and the absorbance at λ = 433 nm was read using a Shimadzu 1800 device. For the blank experiment, MeCN (15 µL) was used in place of the reaction mixture. All the experiments were triplicated (97% identity). In these measurements, the H_2O_2 content is given by:

$\Delta Asample_{(n)} = Ablank - Asample_{(n)}$, (n) being the sample number (eqn 1)

A calibration curve (Fig S9) was independently obtained using the same procedure (1 mm cuvette) and H_2O_2 solutions (prepared by cascade dilutions of commercial 30% H_2O_2 titrated at 9.8 M with the $KMnO_4$ method.[3a] The obtained ΔA values ($\Delta Acal_{(n)}$) were plotted against H_2O_2 concentration in the final sample, $[H_2O_2]_{final\_sample}$(µM), giving the following calibration curve equation:

$[H_2O_2]final\ sample = (\Delta A + 0.0065) / 0.01827$ (eqn2)

Based on eqn. 2, the amount of hydrogen peroxide in the catalytic reactions was determined based on $\Delta Asample_{(n)}$. $[H_2O_2]$ in the reaction mixture was calculated considering the dilution factor:

$[H_2O_2]_{mother\_sample}(\mu M) = [H_2O_2]_{final\_sample} * (2500/15)$ (eqn3)

The results were then confronted to the theoretical $[H_2O_2]$ for a 100% yield and the remaining electron consumption finally attributed to H_2O production.

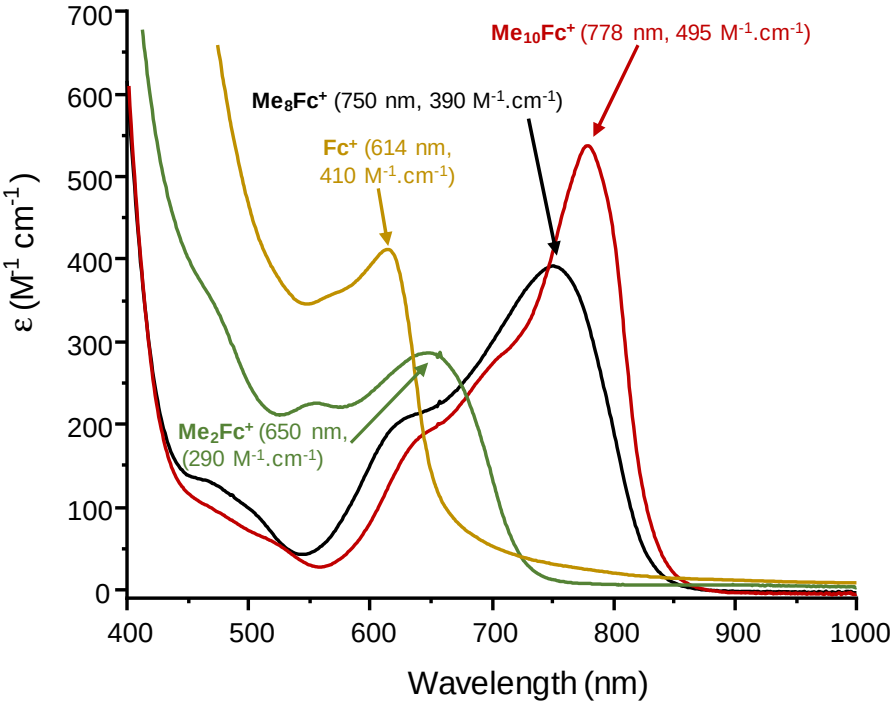

Figure S1. UV-vis spectra of Fc^+, Me_2Fc^+, Me_8Fc^+ and $Me_{10}Fc^+$ in MeCN at 298 K.

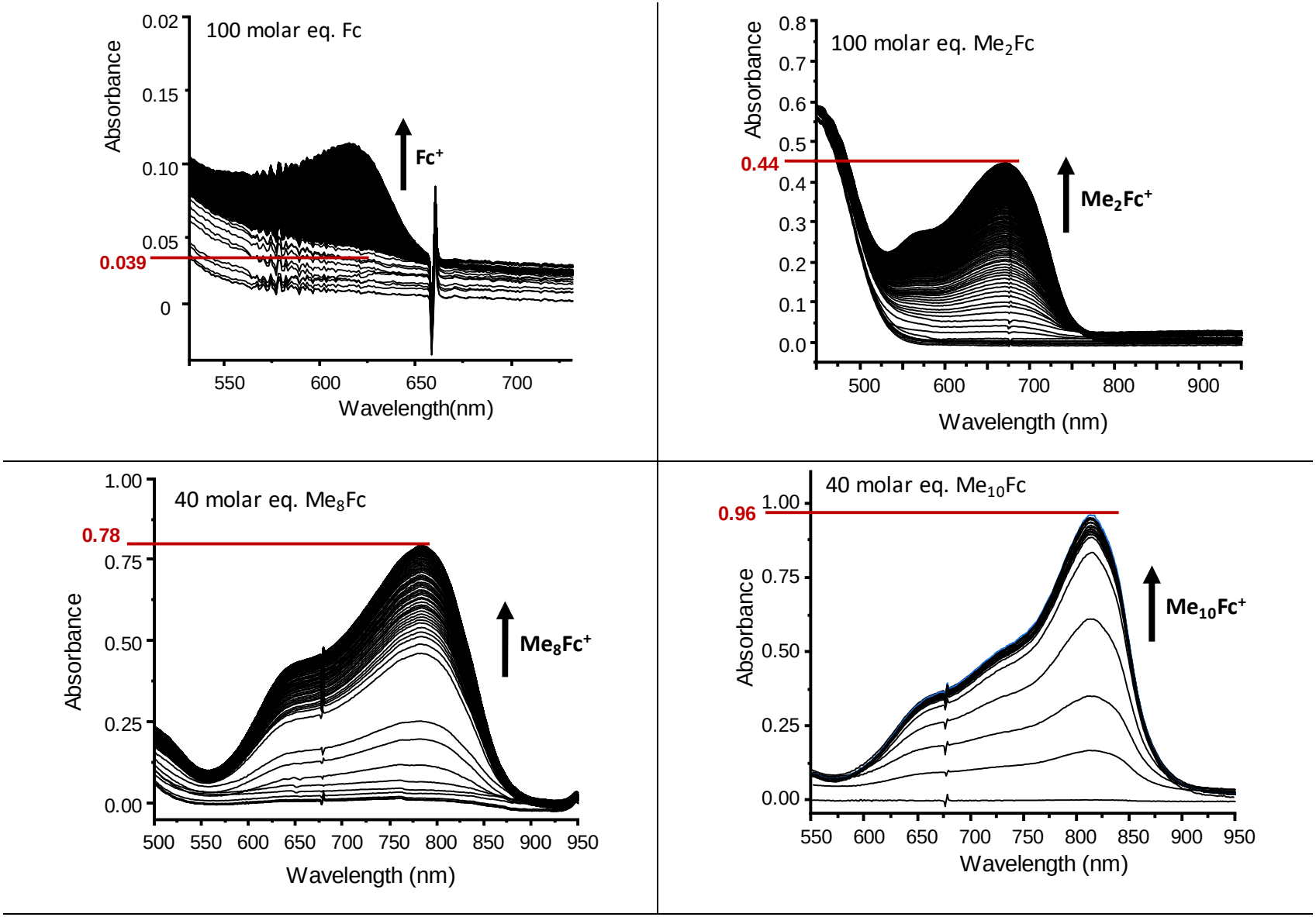

Figure S2. Typical UV-vis changes for the catalytic ORR by **1** in air-saturated MeCN with Fc (100 molar eq.), Me_2Fc (100 molar eq.), Me_8Fc (40 molar eq.) and $Me_{10}Fc$ (40 molar eq.) as electron source and $LutHBF_4$ as proton source. Exp. cond.:[**1**] = 0.5 mM, V = 250 µL, , $n_1 = 1.25 \cdot 10^{-7}$ mole; [$LutHBF_4$] = 2 M, V = 25 µL, $n_{LutHBF4} = 5.0 \cdot 10^{-5}$ mole (400 molar eq.); [Me_2Fc] = [Fc] = 5.6 mM, V = 2.225 mL, $n_{Me2Fc} = n_{Fc} = 1.25 \cdot 10^{-5}$ mole; [Me_8Fc] = [$Me_{10}Fc$] = 2.24 mM, V = 2.225 mL, $n_{Me8Fc} = n_{Me10Fc} = 5.0 \cdot 10^{-6}$ mole; V_{final} = 2.5 mL; T = 298 K; 1 cm path length, Δt = 0.25 s to 1 s; the values in red are discussed in the figures of the corresponding kinetic traces.

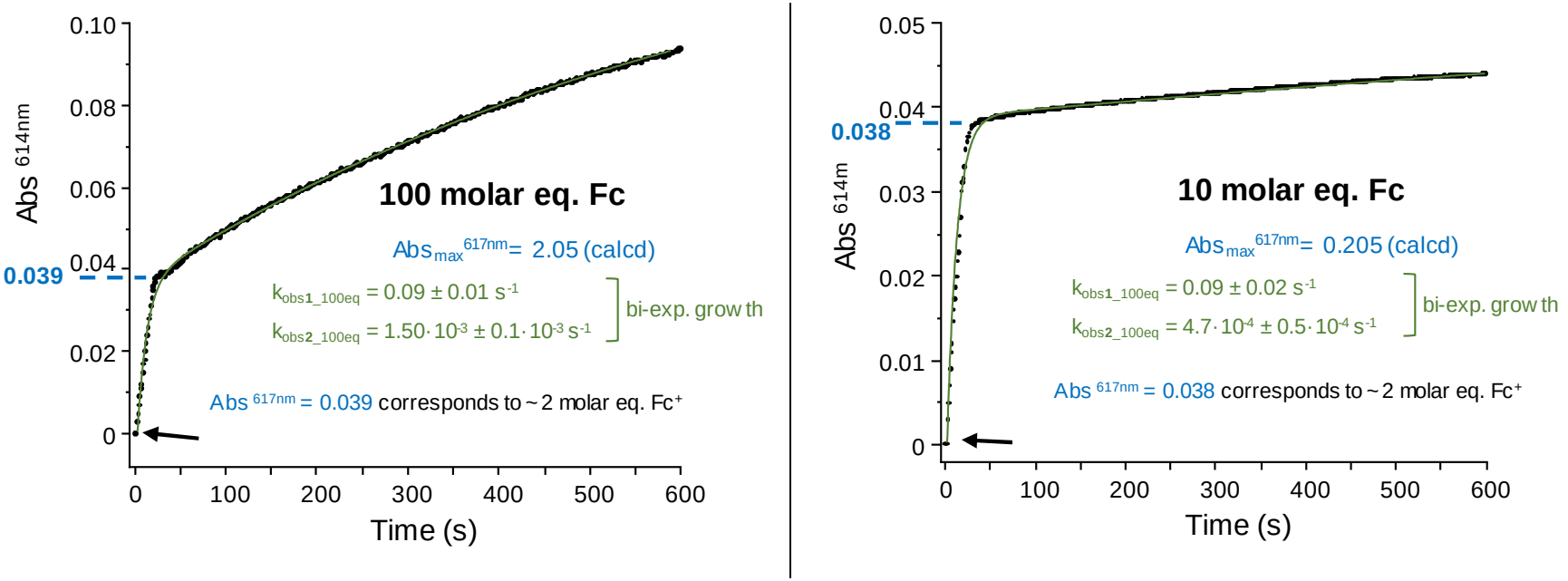

- 2 molar eq. = $2 \times 1.25 \cdot 10^{-7} = 2.5 \cdot 10^{-7}$ mole in a final volume of 2.5 mL, thus giving $[Fc^+] = 0.1$ mM; $\varepsilon_{(Fc+)} = 410\ M^{-1}\ cm^{-1}$ leads to A = 0.041

Figure S3. Kinetic profiles (Abs_{max}^{617nm}) for the catalytic ORR by **1** with $LutHBF_4$ and Fc (10 and 100 molar eq.) in air-saturated MeCN. Exp. cond.: [**1**] = 0.5 mM, V = 250 µL, $n_1 = 1.25 \cdot 10^{-7}$ mole; $[LutHBF_4]$ = 2 M, V = 25 µL, $n_{LutHBF4} = 5.0 \cdot 10^{-5}$ mole (400 molar eq.); $[Fc]_{initial}$ = 0.56 and 5.6 mM, $V_{initial}$ = 2.225 mL giving $n_{Fc} = 1.25 \cdot 10^{-6}$ and $1.25 \cdot 10^{-5}$ mole; V_{final} = 2.5 mL; T = 298 K; 1 cm path length, Δt = 1 s; arrows indicate the injection of **1** in the reaction mixture.

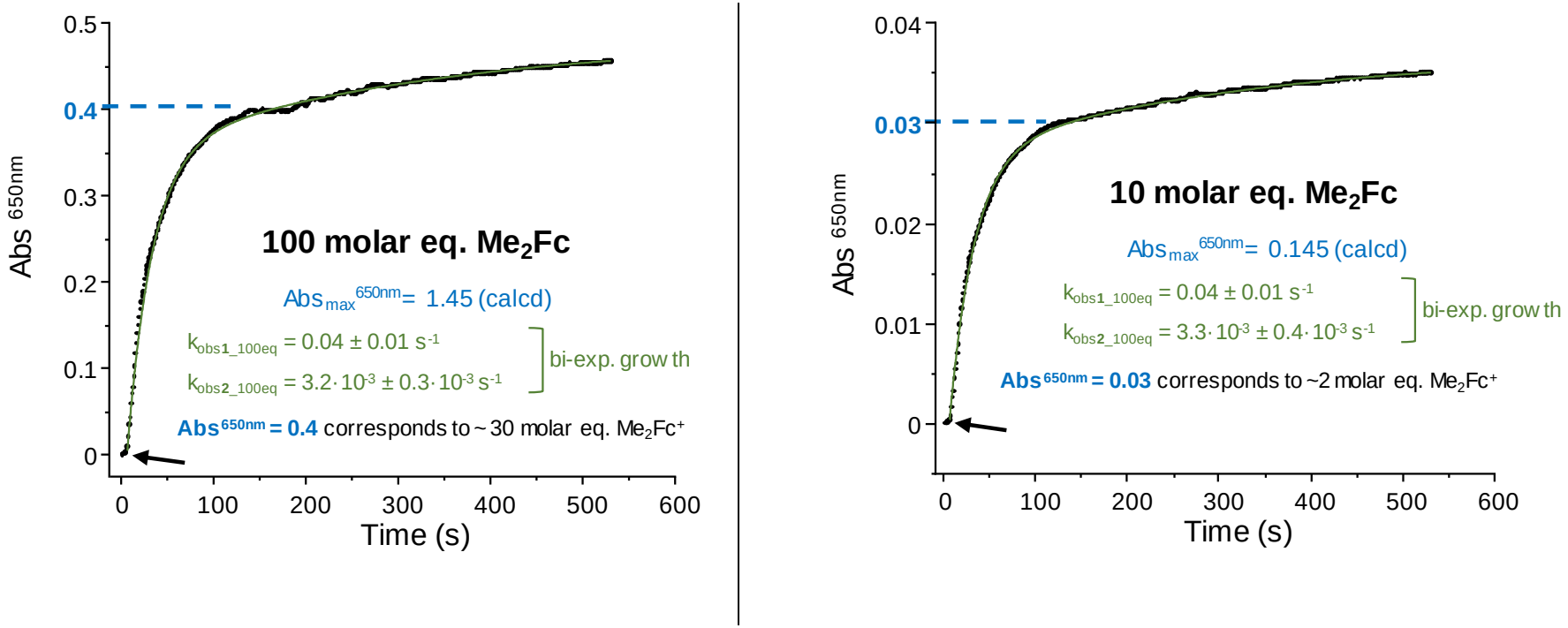

- For 2 molar eq. Me_2Fc^+ = 2 x 1.25x10^{-7} = 2.5 10^{-7} mole in a final volume of 2.5 mL, thus giving [Me_2Fc^+] = 0.1 mM

$\varepsilon_{(Me2Fc+)}$ = 290 M^{-1} cm^{-1} leads to A = 290x1x0.1x10^{-3} = 0.029

- For 30 molar eq. Me_2Fc^+, A = 0.43

Figure S4. Kinetic profiles (Abs_{max}^{650nm}) for the catalytic ORR by **1** with $LutHBF_4$ and Me_2Fc (10 and 100 molar eq.) in air-saturated MeCN. Exp. cond.: [**1**] = 0.5 mM, V = 250 µL, n_1 = 1.25·10^{-7} mole; [$LutHBF_4$] = 2 M, V = 25 µL, $n_{LutHBF4}$ = 5.0·10^{-5} mole (400 molar eq.); $[Me_2Fc]_{initial}$ = 0.56 and 5.6 mM, $V_{initial}$ = 2.225 mL giving n_{Me2Fc} = 1.25·10^{-6} and 1.25·10^{-5}mole; V_{final} = 2.5 mL; T = 298 K; 1 cm path length, Δt = 1 s; arrows indicate the injection of **1** in the reaction mixture.

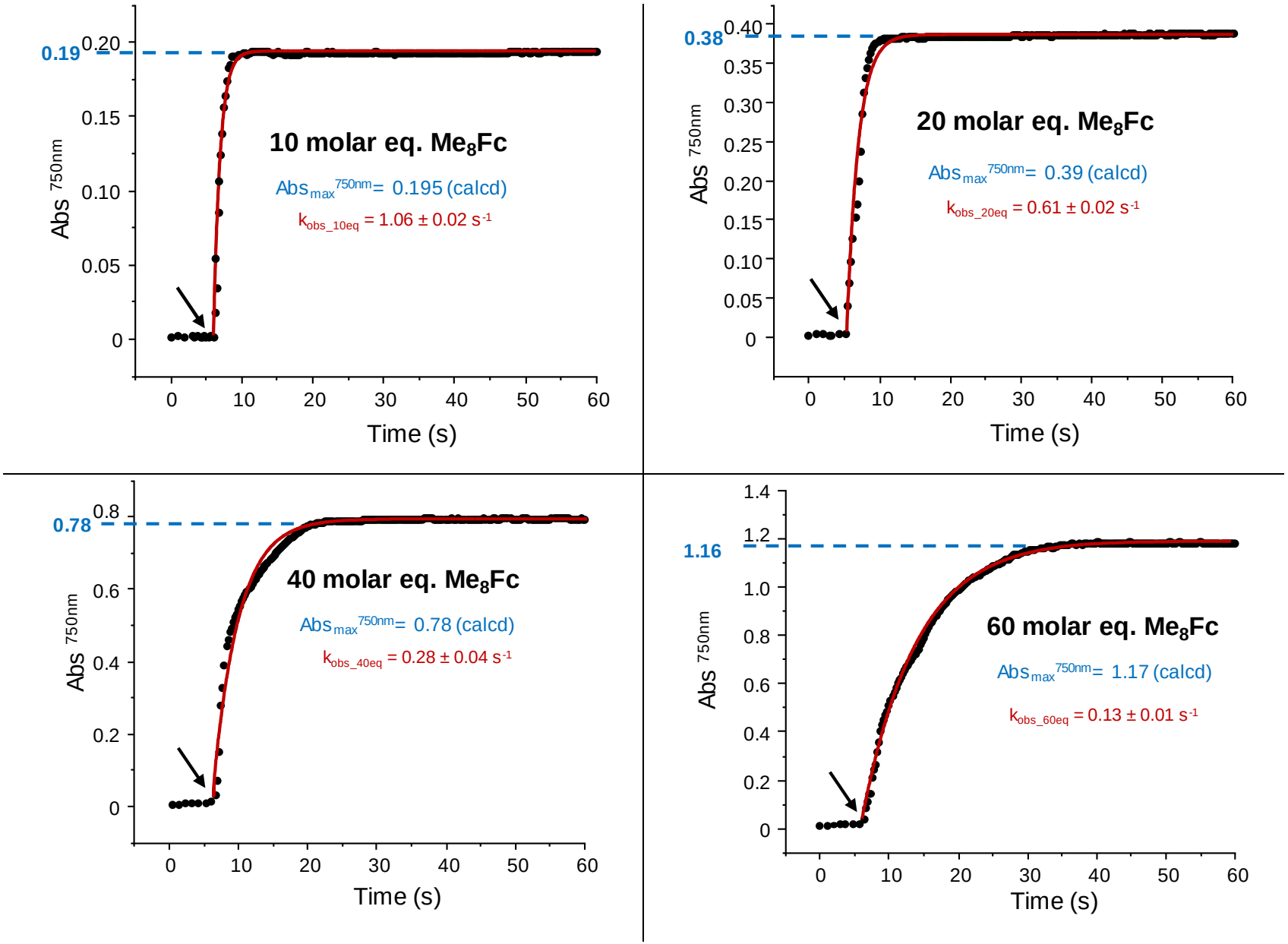

Figure S5. Kinetic profiles (Abs_{max}^{750nm}) for the catalytic ORR by **1** with $LutHBF_4$ and Me_8Fc (10, 20, 40 and 60 molar eq.) in air-saturated MeCN. Exp. cond.: [**1**] = 0.5 mM, V = 250 µL, $n_1 = 1.25 \cdot 10^{-7}$ mole; $[LutHBF_4]$ = 2 M, V = 25 µL, $n_{LutHBF4} = 5.0 \cdot 10^{-5}$ mole (400 molar eq.); $[Me_8Fc]_{initial}$ = 0.56, 1.12, 2.25 and 3.37 mM, $V_{initial}$ = 2.225 mL giving $n_{Me8Fc} = 1.25 \cdot 10^{-6}$, $2.50 \cdot 10^{-6}$, $5.0 \cdot 10^{-6}$ and $7.5 \cdot 10^{-6}$ mole; V_{final} = 2.5 mL; T = 298 K; 1 cm path length, Δt = 0.25 s; arrows indicate the injection of **1** in the reaction mixture.

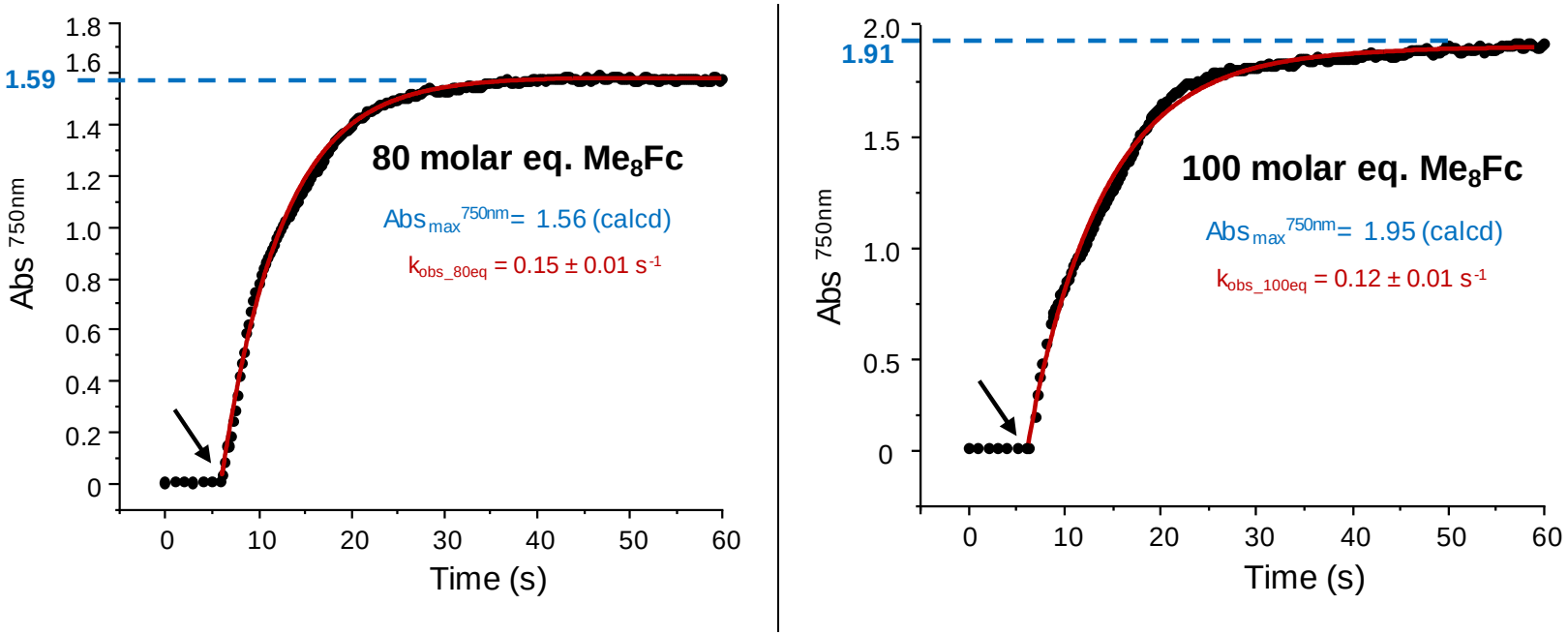

Figure S6. Kinetic profiles (Abs_{max}^{750nm}) for the catalytic ORR by **1** with $LutHBF_4$ and Me_8Fc (80 and 100 molar eq.) in air-saturated MeCN. Exp. cond.: [**1**] = 0.5 mM, V = 250 µL, $n_1 = 1.25 \cdot 10^{-7}$ mole; $[LutHBF_4]$ = 2 M, V = 25 µL, $n_{LutHBF4} = 5.0 \cdot 10^{-5}$ mole (400 molar eq.); $[Me_8Fc]_{initial}$ = 4.49 and 5.6 mM, $V_{initial}$ = 2.225 mL giving $n_{Me8Fc} = 10^{-5}$ and $1.25 \cdot 10^{-5}$ mole); V_{final} = 2.5 mL; T = 298 K; 1 cm path length, Δt = 0.25 s; arrows indicate the injection of **1** in the reaction mixture.

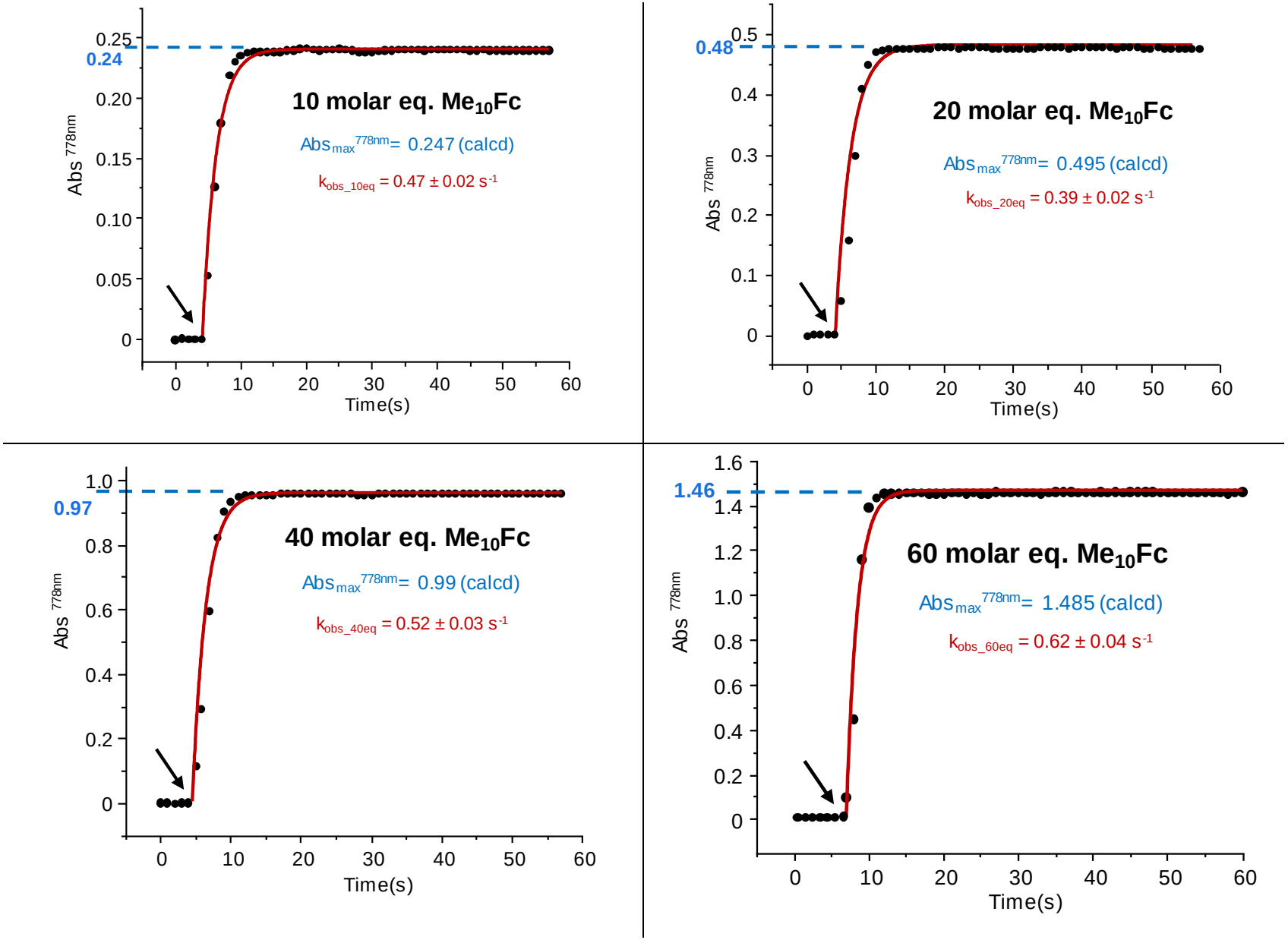

Figure S7. Kinetic profiles (Abs_{max}^{778nm}) for the catalytic ORR by **1** with $LutHBF_4$ and $Me_{10}Fc$ (10, 20, 40 and 60 molar eq.) in air-saturated MeCN. Exp. cond.:[**1**] = 0.5 mM, V = 250 µL, $n_1 = 1.25 \cdot 10^{-7}$ mole; $[LutHBF_4]$ = 2 M, V = 25 µL, $n_{LutHBF4} = 5.0 \cdot 10^{-5}$ mole (400 molar eq.); $[Me_{10}Fc]_{initial}$ = 0.56, 1.12, 2.25 and 3.37 mM, $V_{initial}$ = 2.225 mL giving n_{Me10Fc} = $1.25 \cdot 10^{-6}$, $2.50 \cdot 10^{-6}$, $5.0 \cdot 10^{-6}$ and $7.5 \cdot 10^{-6}$ mole; V_{final} = 2.5 mL; T = 298 K; 1 cm path length, Δt = 1 s; arrows indicate the injection of **1** in the reaction mixture.

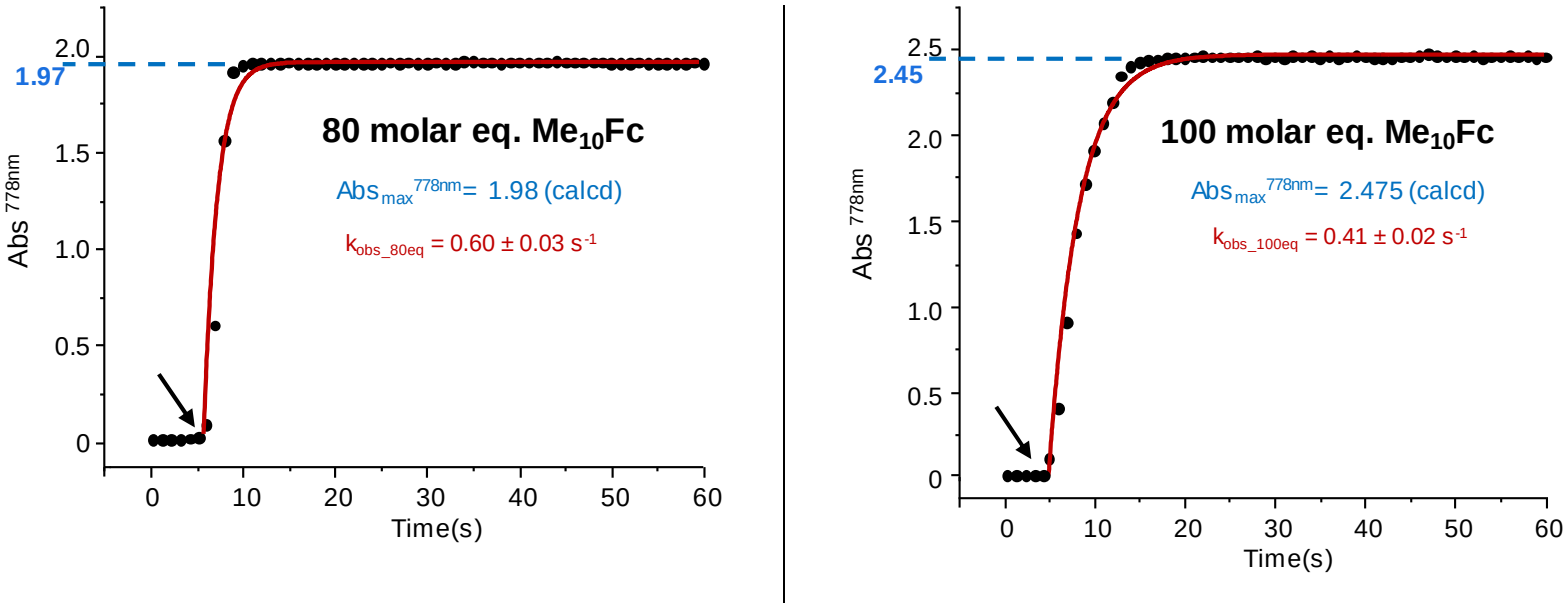

Figure S8. Kinetic profiles (Abs_{max}^{778nm}) for the catalytic ORR by **1** with $LutHBF_4$ and $Me_{10}Fc$ (80 and 100 molar eq.) in air-saturated MeCN. Exp. cond.:[**1**] = 0.5 mM, V = 250 µL, $n_1 = 1.25 \cdot 10^{-7}$ mole; $[LutHBF_4]$ = 2 M, V = 25 µL, $n_{LutHBF4} = 5.0 \cdot 10^{-5}$ mole (400 molar eq.); $[Me_{10}Fc]_{initial}$ = 4.49 and 5.6 mM, $V_{initial}$ = 2.225 mL, $n_{Me10Fc} = 10^{-5}$ and $1.25 \cdot 10^{-5}$ mole); V_{final} = 2.5 mL; T = 298 K; 1 cm path length, Δt = 1 s; arrows indicate the injection of **1** in the reaction mixture.

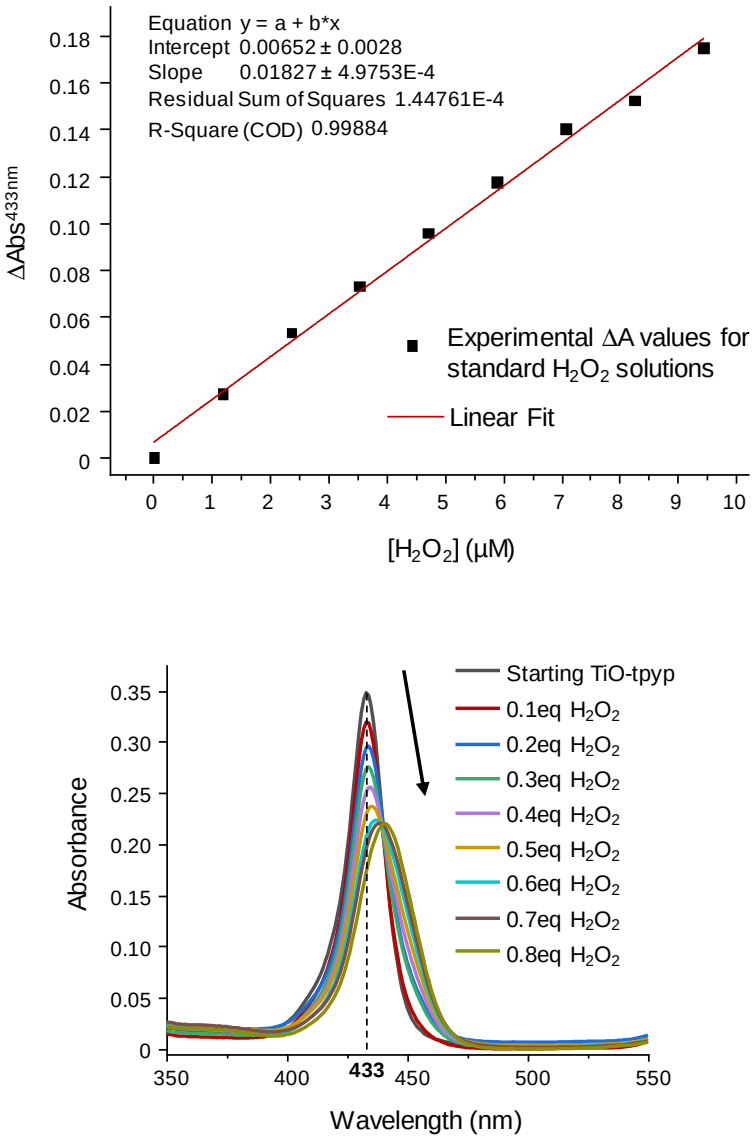

Figure S9. (top) H_2O_2 calibration curve using the TiO-tpyp reagent; (bottom) corresponding UV-vis traces; air-saturated MeCN solutions, 298 K, 1 mm path length.

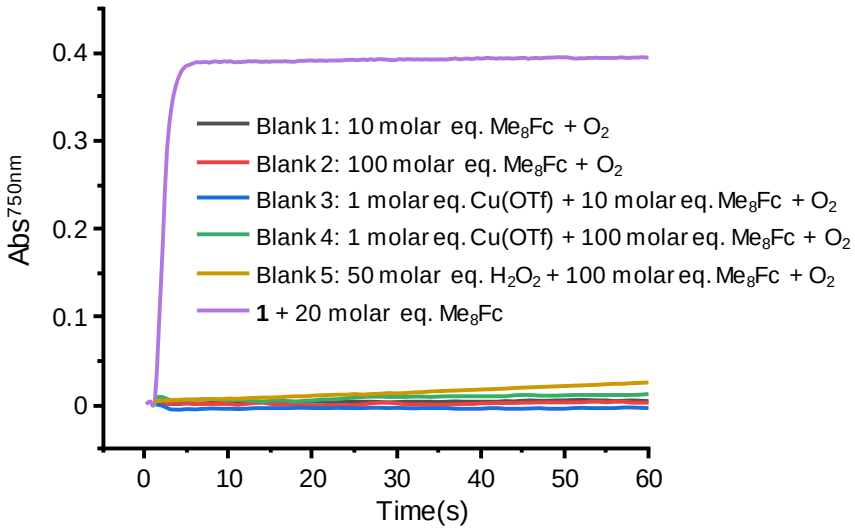

Figure S10. Blank experiments (Blanks 1-5) attesting for the absence of reactivity of Me_8Fc with O_2 (▬ and ▬), Cu(OTf) with Me_8Fc and O_2 (▬ and ▬), H_2O_2 + Me_8Fc +O_2 (▬) compared to **1** (▬); *Blank 1:* 250 µL MeCN + 2.225 mL Me_8Fc (0.56 mM), 25 µl $LutHBF_4$ (2 M); *Blank 2:* 250 µL MeCN + 2.225 mL Me_8Fc (5.6 mM), 25 µl $LutHBF_4$ (2 M); *Blank 3:* 250 µL Cu(OTf) (0.5 mM in MeCN) + 2.225 mL Me_8Fc (0.56 mM), 25 µl $LutHBF_4$ (2 M); *Blank 4:* 250 µL Cu(OTf) (0.5 mM in MeCN) + 2.225 mL Me_8Fc (5.6 mM), 25 µL$LutHBF_4$ (2 M); *Blank 5:* 250 µL H_2O_2 (25 mM) + 2.225 mL Me_8Fc (5.6 mM), 25 µL $LutHBF_4$ (2 M); V_{final} = 2.5 mL; T = 298 K; air-saturated MeCN solutions. Me_8Fc^+ accumulation is only detected in the presence of **1** (increase in absorbance at 750 nm).

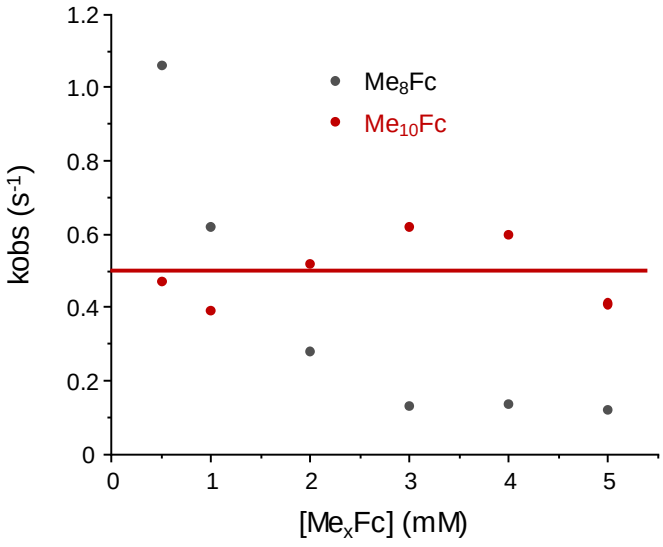

Figure S11. Plot of the *pseudo*-first-order rate constants (k_{obs}) *versus* [Me_xFc] for the ORR catalysed by **1** in the presence of 400 molar eq. $LutHBF_4$ in air-saturated MeCN at 298 K.

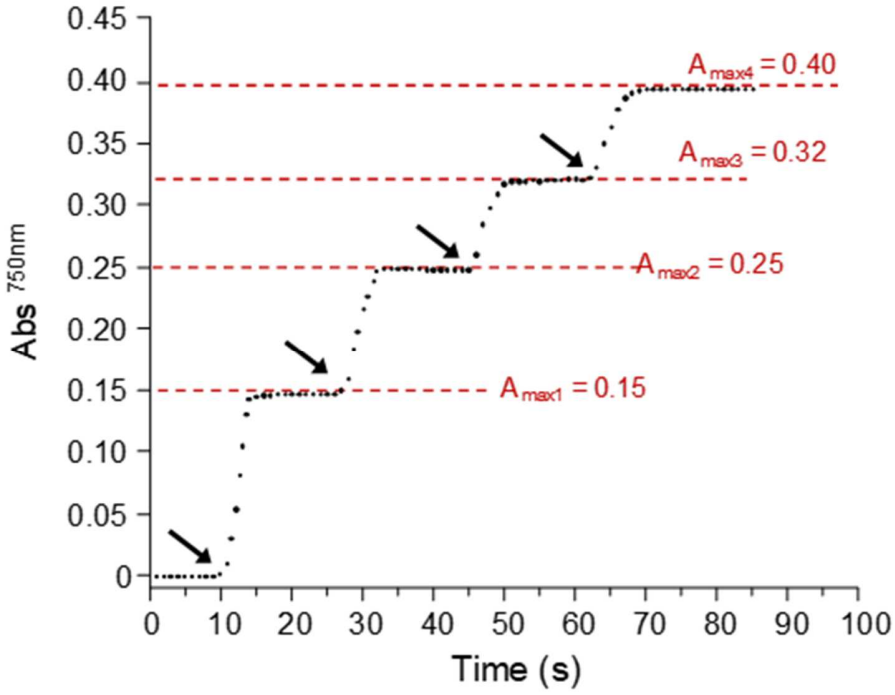

Figure S12. Me_8Fc^+ accumulation (by monitoring the absorbance at 750 nm) upon successive runs under H_2O_2 production conditions. Arrows indicate Me_8Fc injection (10 molar eq.) and the dotted red lines the theoretical absorbance values for each run, taking into account dilution factors. Exp. cond.: [**1**] = 0.05 mM, **1** /Me_8Fc/LutHBF$_4$ at 1/10/400, air-saturated MeCN, 298 K.

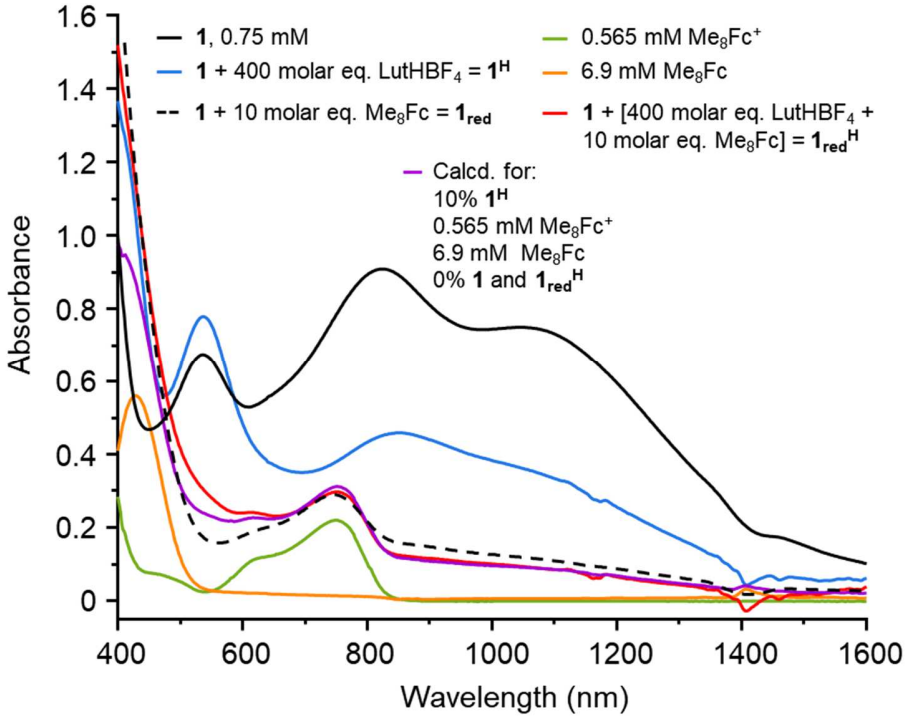

Figure S13. Changes in the UV-vis/NIR spectrum of **1** (0.75 mM) in the presence of proton and electron sources under inert atmosphere; MeCN, 298 K, path length = 1 cm.

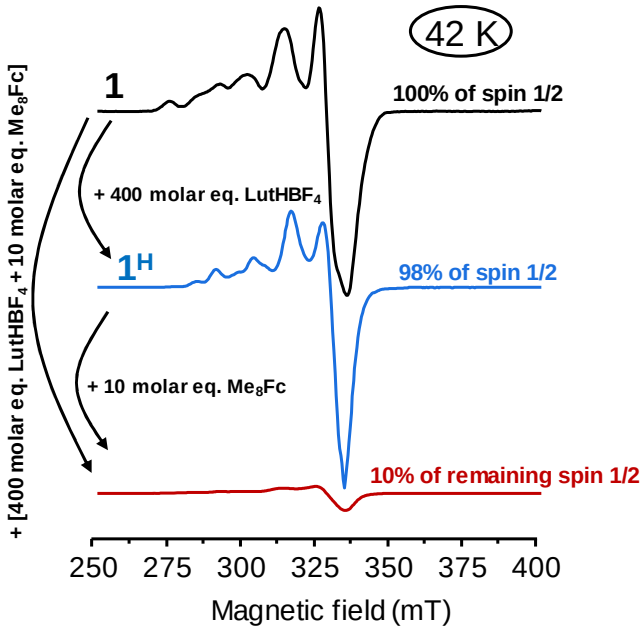

Figure S14. Changes in the X-band (9.39 GHz) EPR spectrum of **1** (black) upon the subsequent reaction with $LutHBF_4$ (400 molar eq., blue) and Me_8Fc (10 molar eq., red) or a mixture of both reagents in MeCN and under inert atmosphere at 42 K; **[1]** = 0. 75 mM; power 0.25 mW; mod. ampl. 1 mT; mod. freq. 100 kHz.

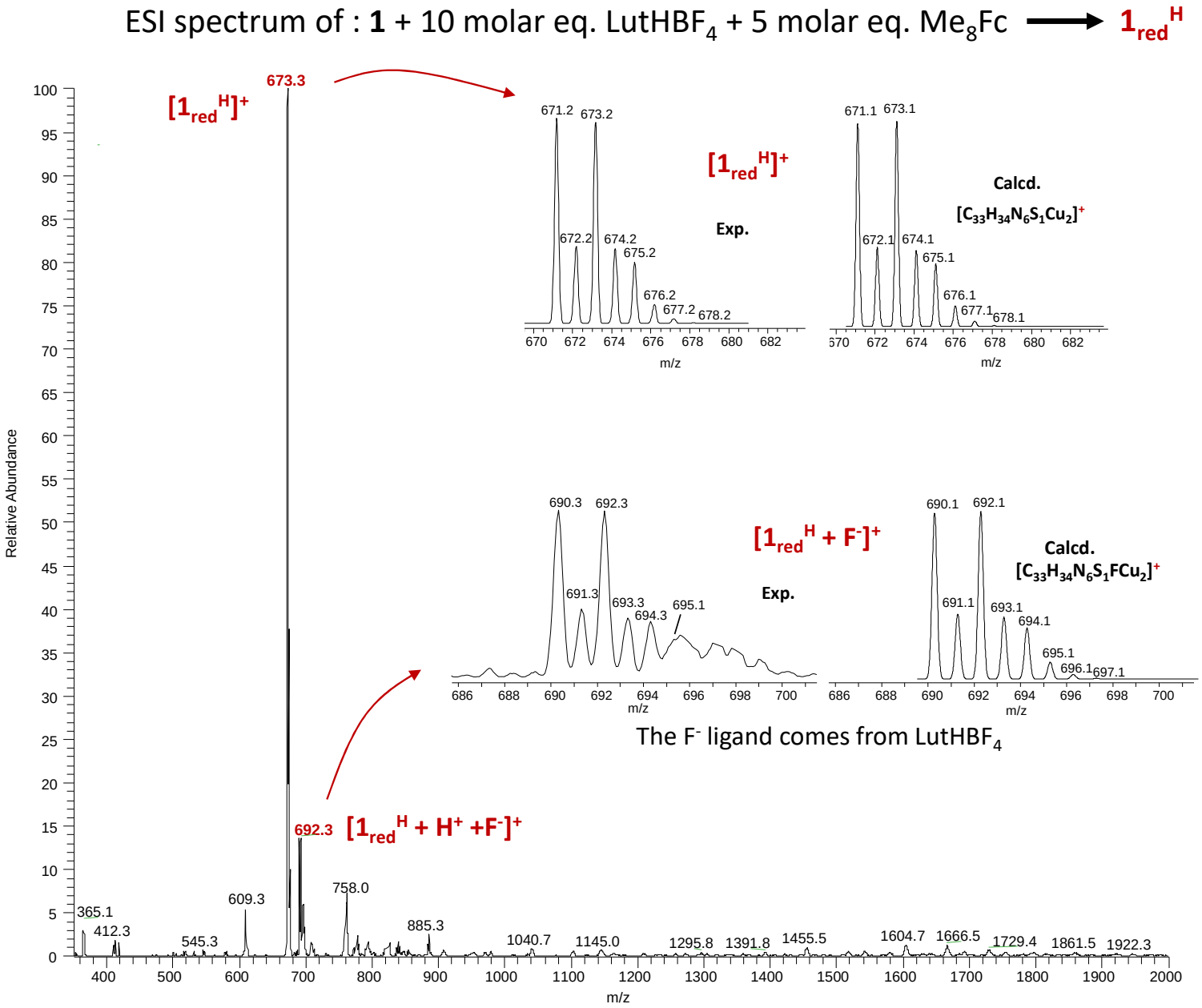

Figure S15. Electrospray ionization mass spectrum of *in situ* generated $\mathbf{1}_{red}^{H}$ from the reaction of **1** with $LutHBF_4$ and Me_8Fc in MeCN.

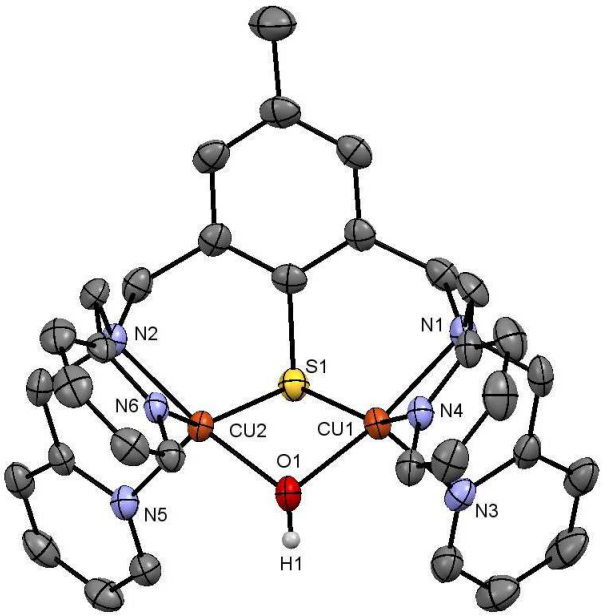

Figure S16. ORTEP diagram of dicationic $\mathbf{1_{ox}}^{2+}$ with all non-H atoms shown as 50% thermal ellipsoids. Selected interatomic distances (Å) and angles (deg): Cu1-Cu2, 2.9238(5); Cu1-S1, 2.3447(9); Cu1-N1, 2.082(3); Cu1-N3, 2.150(3); Cu1-N4, 2.029(3); Cu2-S1, 2.3728(10); Cu2-N2, 2.071(3); Cu1-N5, 2.176(3); Cu1-N6, 2.014(3); Cu1-S1-Cu2, 76.60(3); Cu1-O1-Cu2, 97.82(11). CCDC deposition number 2014256, see Tables S3 and S4 for additional details.

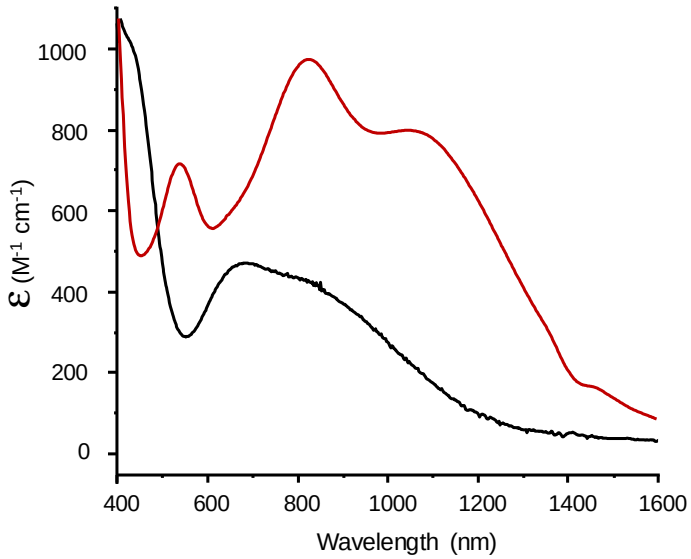

Figure S17. UV-vis/NIR spectra of **1** before (red) and after ($\mathbf{1_{ox}}$, black) exposure to air in MeCN at 298 K.

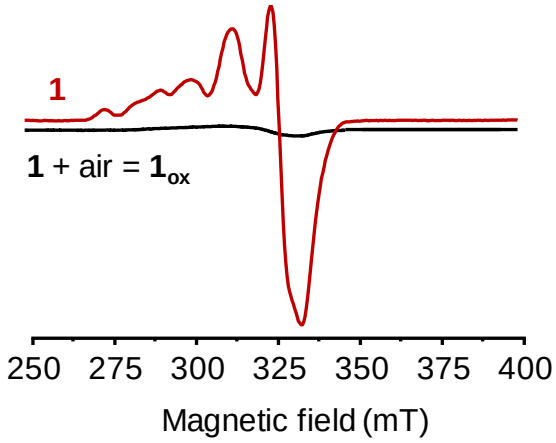

Figure S18. Changes in the X-band (9.39 GHz) EPR spectrum of **1** before (red) and after (black, $\mathbf{1}_{ox}$) exposure to air in MeCN at 42 K; **[1]** = 0. 75 mM, power 0.25 mW; mod. ampl. 1 mT; mod. freq. 100 kHz.

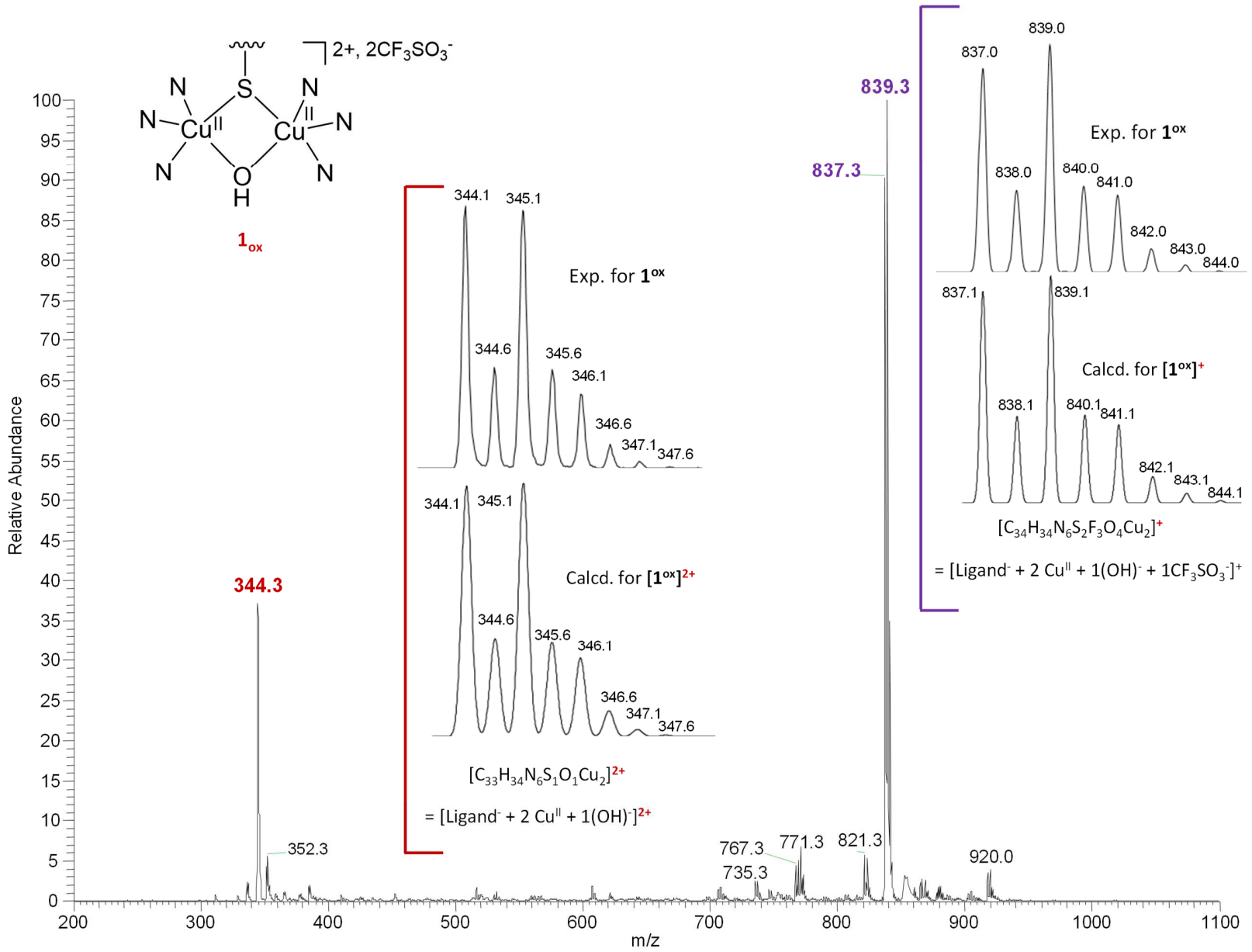

Figure S19. Electrospray ionization mass spectrum of $\mathbf{1_{ox}}$ generated from air oxidation of a MeCN solution of **1**.

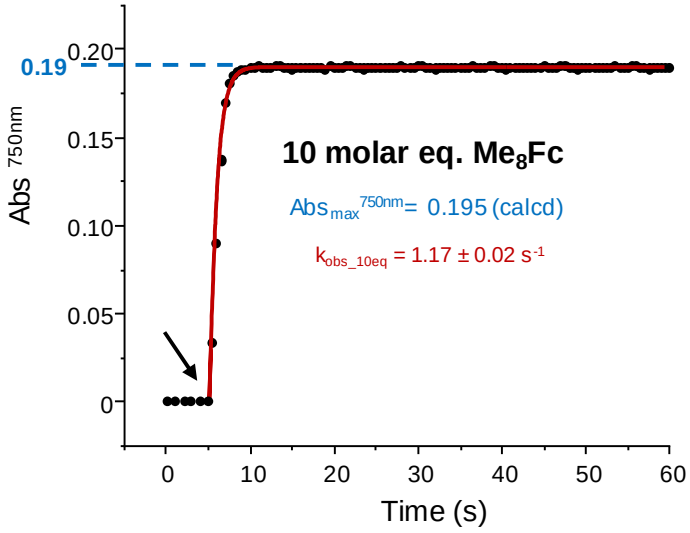

Figure S20. Kinetic profiles (Abs_{max}^{750nm}) resulting from the reaction of $\mathbf{1^{ox}}$ with an air-saturated MeCN mixture of Me_8Fc and $LutHBF_4$ (1/10/400). Exp. cond.: $\mathbf{[1_{ox}]}$ = 0.5 mM, V = 250 µL, $n_1 = 1.25 \cdot 10^{-7}$ mole; $[Me_8Fc]_{initial}$ = 0.56 mM, $V_{initial}$ = 2.225 mL; $n_{Me8Fc} = 1.25 \cdot 10^{-6}$ mole; $[LutHBF_4]$ = 2 M,V = 25 µL, $n_{LutHBF4} = 5.0 \cdot 10^{-5}$ mole (400 molar eq.); V_{final} = 2.5 mL; T = 298 K; 1 cm path length, Δt = 0.5 s.

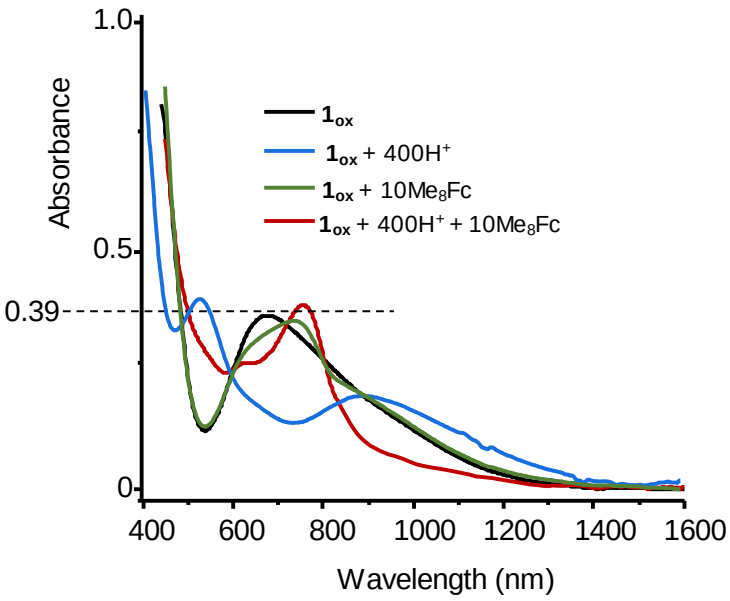

Figure S21. Changes in the UV-vis spectrum of $\mathbf{1_{ox}}$ (0.5 mM) consecutive to the addition of $LutHBF_4$, Me_8Fc or a combination under inert atmosphere in MeCN at 298 K; path length = 1 cm. The theoretical value of 0.39 in absorbance corresponds to a quantitative $2e^-$ reduction of $\mathbf{1_{ox}}$ or $\mathbf{1_{ox}^H}$.

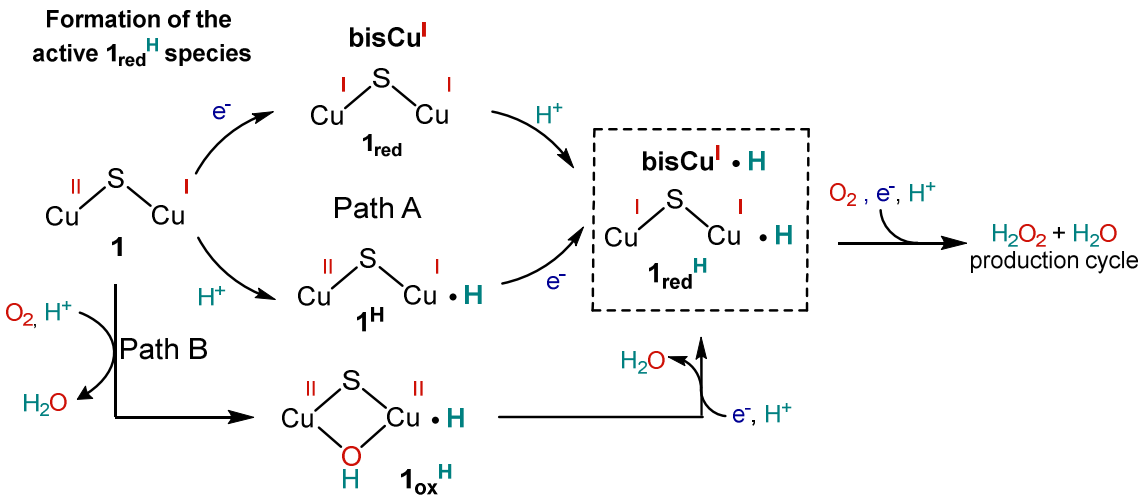

Figure S22. Possible routes for the formation of $\mathbf{1}_{red}^{H}$ starting from **1**.

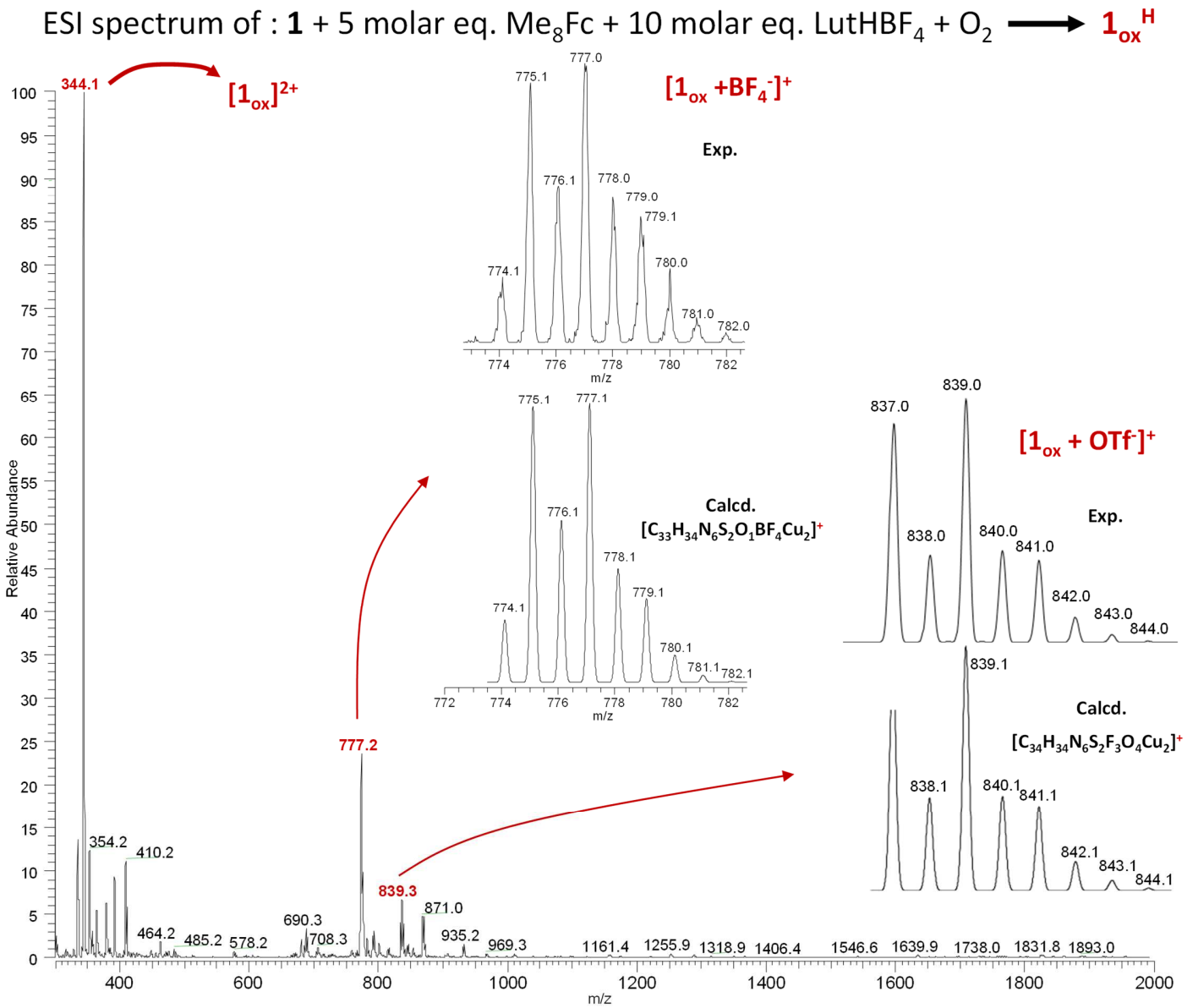

Figure S23. Electrospray ionization mass spectrum of the final reaction mixture obtained upon air exposure of a combination of **1** + $LutHBF_4$ and Me_8Fc in MeCN. Deprotonation processes are likely to occur in the ionization chamber.

Table S1. Calculated maximum absorbance values for the tested experimental conditions.[a]

	Fc^+ λ_{max} = 614 nm; ε = 410 M^{-1} cm^{-1}	Me_2Fc^+ λ_{max} = 650 nm; ε = 290 M^{-1} cm^{-1}	Me_8Fc^+ λ_{max} = 750 nm; ε = 390 M^{-1} cm^{-1}	$Me_{10}Fc^+$ λ_{max} = 778 nm; ε = 495 M^{-1} cm^{-1}
10 molar eq.	0.205	0.145	0.195	0.247
20 molar eq	-[b]	-[b]	0.390	0.495
40 molar eq.	-[b]	-[b]	0.780	0.990
60 molar eq.	-[b]	-[b]	1.170	1.485
80 molar eq	-[b]	-[b]	1.560	1.980
100 molar eq.	2.050	1.450	1.950	2.475

[a]Exp. cond.: **[1]** = 0.5 mM, $V_{[1]}$ = 250µL, $n_1 = 1.25 \cdot 10^{-7}$ mole; n_{MexFc} (x = 0, 2, 8 and 10)= $1.25 \cdot 10^{-6}$, $2.5 \cdot 10^{-6}$, $5.0 \cdot 10^{-6}$, $7.50 \cdot 10^{-6}$, 10^{-5} and $1.25 \cdot 10^{-5}$ mole in 2.225 mL leads to $[Me_xFc]_{initial}$ = 0.56, 1.12, 2.24, 3.37, 4.49 and 5.6 mM in $V_{initial}$ = 2.225 mL. Given V_{final} = 2.225 (Me_xFc) + 0.250 (**1**) + 0.025 ($LutHBF_4$) = 2.5 mL, the dilution factor is 0.89. This leads to $[Me_xFc]_{final}$ = 0.50, 1.0, 2.0, 3.0, 4.0 and 5.0 mM used for the calculations; [b]Conditions not tested.

Table S2. k_{obs} (s^{-1}) values obtained from mono- (red) or bi-exponential (green) fits of the kinetics traces corresponding to the accumulation of ferrocenium derivatives at the appropriate λ_{max}.

	10 molar eq. 0.5 mM	20 molar eq. 1.0 mM	40 molar eq. 2.0 mM	60 molar eq. 3.0 mM	80 molar eq. 4.0 mM	100 molar eq. 5.0 mM
k_{obs} Fc^+	0.09 ± 0.02 $4.7 \cdot 10^{-4} \pm 0.5 \cdot 10^{-4}$	-[a]	-[a]	-[a]	-[a]	0.09 ± 0.01 $1.5 \cdot 10^{-3} \pm 0.1 \cdot 10^{-3}$
k_{obs} Me_2Fc^+	0.040 ± 0.01 $3.3 \cdot 10^{-3} \pm 0.4. \cdot 10^{-3}$	-[a]	-[a]	-[a]	-[a]	0.04 ± 0.01 $3.2 \cdot 10^{-3} \pm 0.3 \cdot 10^{-3}$
k_{obs} Me_8Fc^+	1.06 ± 0.02	0.61 ± 0.02	0.28 ± 0.04	0.13 ± 0.01	0.15 ± 0.01	0.12 ± 0.01
k_{obs} $Me_{10}Fc^+$	0.47 ± 0.02	0.39 ± 0.02	0.52 ± 0.03	0.62 ± 0.04	0.60 ± 0.03	0.41 ± 0.02

[a]: not measured

Table S3. Crystal data and structure refinement for $\mathbf{1_{ox}}$.

Empirical formula	$\mathbf{C_{38}\ H_{42}\ Cl_6\ Cu_2\ F_6\ N_6\ O_8\ S_3}$
Formula weight	1260.74
Temperature	150(2) K
Wavelength	0.71073 Å
Crystal system	Triclinic
Space group	$P\ ^{-1}$
Unit cell dimensions	a = 12.9903(4) Å α = 74.072(3)°
	b = 14.2793(5) Å β = 66.275(3)°
	c = 15.5742(6) Å γ = 86.862(3)°
Volume, Z	2538.12(15) $Å^3$, 2
Density (calculated)	1.650 g/cm^3
Absorption coefficient	1.353 mm^{-1}
F(000)	1276
Crystal size	0.20 x 0.08 x 0.08 mm
θ range for data collection	2.97 to 26.37°
Limiting indices	-16<=h<=16, -17<=k<=17, -19<=l<=19
Reflections collected	34311
Independent reflections	10358 [R(int) = 0.0389]
Absorption correction	Semi-empirical from equivalents
Max. and min. transmission	0.8995 and 0.7736
Refinement method	Full-matrix least-squares on F^2
Data / Restraints / Parameters	10358 / 0 / 818
Goodness-of-fit on F^2	0.908
Final R indices [I>2σ(I)]	R1 = 0.0426, wR2 = 0.1043
R indices (all data)	R1 = 0.0691, wR2 = 0.1093

Table S4. Bond length [Å] and angles [deg] for $\mathbf{1_{ox}}$.

Cu(1)-Cu(2)	2.9238(5)	C(12)-H(12)	0.99(4)
Cu(1)-O(1)	1.944(2)	C(13)-C(14)	1.387(7)
Cu(1)-N(4)	2.029(3)	C(13)-H(13)	0.80(5)
Cu(1)-N(1)	2.082(3)	C(14)-C(15)	1.378(6)
Cu(1)-N(3)	2.150(3)	C(14)-H(14)	0.95(4)
Cu(1)-S(1)	2.3447(9)	C(15)-H(15)	0.91(3)
Cu(2)-O(1)	1.935(2)	C(16)-C(17)	1.496(5)
Cu(2)-N(6)	2.014(3)	C(16)-H(16A)	0.95(3)
Cu(2)-N(2)	2.071(3)	C(16)-H(16B)	0.99(3)
Cu(2)-N(5)	2.176(3)	C(17)-C(18)	1.382(5)
Cu(2)-S(1)	2.3728(10)	C(18)-C(19)	1.377(6)
S(1)-C(1)	1.775(4)	C(18)-H(18)	0.84(3)
O(1)-H(1O)	0.78(4)	C(19)-C(20)	1.374(6)
N(1)-C(16)	1.471(5)	C(19)-H(19)	0.96(4)
N(1)-C(10)	1.499(5)	C(20)-C(21)	1.377(5)
N(1)-C(8)	1.514(4)	C(20)-H(20)	0.80(4)
N(2)-C(28)	1.476(5)	C(21)-H(21)	0.85(3)
N(2)-C(22)	1.497(4)	C(22)-C(23)	1.493(5)
N(2)-C(9)	1.504(4)	C(22)-H(22A)	0.97(3)
N(3)-C(15)	1.335(5)	C(22)-H(22B)	0.85(3)
N(3)-C(11)	1.351(4)	C(23)-C(24)	1.379(5)
N(4)-C(21)	1.327(5)	C(24)-C(25)	1.357(6)
N(4)-C(17)	1.345(4)	C(24)-H(24)	0.83(4)
N(5)-C(27)	1.332(5)	C(25)-C(26)	1.370(6)
N(5)-C(23)	1.346(4)	C(25)-H(25)	0.88(4)
N(6)-C(33)	1.342(4)	C(26)-C(27)	1.377(5)
N(6)-C(29)	1.350(4)	C(26)-H(26)	0.78(4)
C(1)-C(6)	1.390(5)	C(27)-H(27)	0.85(3)
C(1)-C(2)	1.394(5)	C(28)-C(29)	1.500(5)
C(2)-C(3)	1.391(5)	C(28)-H(28A)	0.94(4)
C(2)-C(8)	1.522(5)	C(28)-H(28B)	0.94(4)
C(3)-C(4)	1.385(5)	C(29)-C(30)	1.378(5)
C(3)-H(3)	0.83(4)	C(30)-C(31)	1.379(6)
C(4)-C(5)	1.375(5)	C(30)-H(30)	0.92(4)
C(4)-C(7)	1.508(6)	C(31)-C(32)	1.379(6)
C(5)-C(6)	1.396(5)	C(31)-H(31)	0.98(4)
C(5)-H(5)	0.89(4)	C(32)-C(33)	1.363(5)
C(6)-C(9)	1.509(5)	C(32)-H(32)	0.83(4)
C(7)-H(7A)	0.94(5)	C(33)-H(33)	0.85(3)
C(7)-H(7B)	1.07(5)	C(41)-Cl(1)	1.764(5)
C(7)-H(7C)	0.82(6)	C(41)-Cl(2)	1.782(5)
C(8)-H(8A)	0.92(4)	C(41)-H(41A)	1.00(4)
C(8)-H(8B)	1.01(4)	C(41)-H(41B)	0.97(4)
C(9)-H(9A)	0.97(3)	C(42)-Cl(4)	1.620(11)
C(9)-H(9B)	0.86(4)	C(42)-Cl(3)	1.651(9)
C(10)-C(11)	1.503(6)	C(42)-Cl(3B)	1.743(8)
C(10)-H(10A)	0.92(3)	C(42)-Cl(4B)	1.802(7)
C(10)-H(10B)	0.90(4)	C(42)-H(42A)	0.9900
C(11)-C(12)	1.383(5)	C(42)-H(42B)	0.9900
C(12)-C(13)	1.367(7)	C(43A)-Cl(5)	1.699(14)

C(43A)-Cl(6)	1.699(15)	C(1)-S(1)-Cu(1)	99.00(12)
C(43A)-H(43A)	0.9900	C(1)-S(1)-Cu(2)	97.49(12)
C(43A)-H(43B)	0.9900	Cu(1)-S(1)-Cu(2)	76.60(3)
C(43B)-Cl(5B)	1.721(9)	Cu(2)-O(1)-Cu(1)	97.82(11)
C(43B)-Cl(6B)	1.757(11)	Cu(2)-O(1)-H(1O)	122(3)
C(43B)-H(43C)	0.9900	Cu(1)-O(1)-H(1O)	119(3)
C(43B)-H(43D)	0.9900	C(16)-N(1)-C(10)	109.6(3)
O(2)-H(1O2)	0.90(5)	C(16)-N(1)-C(8)	110.9(3)
O(2)-H(2O2)	0.81(5)	C(10)-N(1)-C(8)	109.2(3)
S(2)-O(3S2)	1.408(3)	C(16)-N(1)-Cu(1)	106.9(2)
S(2)-O(2S2)	1.423(3)	C(10)-N(1)-Cu(1)	105.8(2)
S(2)-O(1S2)	1.443(4)	C(8)-N(1)-Cu(1)	114.3(2)
S(2)-C(2S)	1.788(5)	C(28)-N(2)-C(22)	108.7(3)
F(1S2)-C(2S)	1.284(6)	C(28)-N(2)-C(9)	111.5(3)
F(2S2)-C(2S)	1.289(6)	C(22)-N(2)-C(9)	108.8(3)
F(3S2)-C(2S)	1.345(8)	C(28)-N(2)-Cu(2)	108.4(2)
S(3)-O(3S3)	1.383(3)	C(22)-N(2)-Cu(2)	105.8(2)
S(3)-O(1S3)	1.415(4)	C(9)-N(2)-Cu(2)	113.5(2)
S(3)-O(2S3)	1.416(3)	C(15)-N(3)-C(11)	118.8(3)
S(3)-C(3S)	1.784(5)	C(15)-N(3)-Cu(1)	129.1(3)
F(1S3)-C(3S)	1.273(6)	C(11)-N(3)-Cu(1)	110.6(2)
F(2S3)-C(3S)	1.300(6)	C(21)-N(4)-C(17)	119.5(3)
F(3S3)-C(3S)	1.331(6)	C(21)-N(4)-Cu(1)	125.4(2)
O(1)-Cu(1)-N(4)	93.48(11)	C(17)-N(4)-Cu(1)	114.8(2)
O(1)-Cu(1)-N(1)	169.07(12)	C(27)-N(5)-C(23)	118.3(3)
N(4)-Cu(1)-N(1)	80.77(11)	C(27)-N(5)-Cu(2)	128.6(2)
O(1)-Cu(1)-N(3)	107.82(11)	C(23)-N(5)-Cu(2)	109.0(2)
N(4)-Cu(1)-N(3)	109.40(11)	C(33)-N(6)-C(29)	118.8(3)
N(1)-Cu(1)-N(3)	82.94(11)	C(33)-N(6)-Cu(2)	125.0(2)
O(1)-Cu(1)-S(1)	85.60(7)	C(29)-N(6)-Cu(2)	115.7(2)
N(4)-Cu(1)-S(1)	153.31(9)	C(6)-C(1)-C(2)	119.8(3)
N(1)-Cu(1)-S(1)	95.36(8)	C(6)-C(1)-S(1)	119.8(3)
N(3)-Cu(1)-S(1)	96.17(8)	C(2)-C(1)-S(1)	120.4(3)
O(1)-Cu(1)-Cu(2)	40.98(7)	C(3)-C(2)-C(1)	118.8(3)
N(4)-Cu(1)-Cu(2)	112.81(8)	C(3)-C(2)-C(8)	120.5(3)
N(1)-Cu(1)-Cu(2)	133.32(8)	C(1)-C(2)-C(8)	120.6(3)
N(3)-Cu(1)-Cu(2)	127.26(8)	C(4)-C(3)-C(2)	122.3(4)
S(1)-Cu(1)-Cu(2)	52.14(2)	C(4)-C(3)-H(3)	126(3)
O(1)-Cu(2)-N(6)	92.96(11)	C(2)-C(3)-H(3)	112(3)
O(1)-Cu(2)-N(2)	170.54(11)	C(5)-C(4)-C(3)	117.9(4)
N(6)-Cu(2)-N(2)	81.41(11)	C(5)-C(4)-C(7)	119.2(4)
O(1)-Cu(2)-N(5)	106.90(11)	C(3)-C(4)-C(7)	122.9(4)
N(6)-Cu(2)-N(5)	114.40(11)	C(4)-C(5)-C(6)	121.5(4)
N(2)-Cu(2)-N(5)	82.42(11)	C(4)-C(5)-H(5)	116(2)
O(1)-Cu(2)-S(1)	85.01(8)	C(6)-C(5)-H(5)	122(2)
N(6)-Cu(2)-S(1)	146.95(8)	C(1)-C(6)-C(5)	119.7(3)
N(2)-Cu(2)-S(1)	95.55(8)	C(1)-C(6)-C(9)	121.1(3)
N(5)-Cu(2)-S(1)	97.60(8)	C(5)-C(6)-C(9)	119.3(3)
O(1)-Cu(2)-Cu(1)	41.20(7)	C(4)-C(7)-H(7A)	112(3)
N(6)-Cu(2)-Cu(1)	108.81(7)	C(4)-C(7)-H(7B)	113(2)
N(2)-Cu(2)-Cu(1)	133.79(8)	H(7A)-C(7)-H(7B)	103(4)
N(5)-Cu(2)-Cu(1)	127.25(8)	C(4)-C(7)-H(7C)	114(5)
S(1)-Cu(2)-Cu(1)	51.27(2)	H(7A)-C(7)-H(7C)	118(5)

H(7B)-C(7)-H(7C)	96(5)	N(4)-C(21)-H(21)	114(2)
N(1)-C(8)-C(2)	113.7(3)	C(20)-C(21)-H(21)	125(2)
N(1)-C(8)-H(8A)	109(2)	C(23)-C(22)-N(2)	111.2(3)
C(2)-C(8)-H(8A)	109(2)	C(23)-C(22)-H(22A)	113(2)
N(1)-C(8)-H(8B)	109(2)	N(2)-C(22)-H(22A)	108.9(19)
C(2)-C(8)-H(8B)	109(2)	C(23)-C(22)-H(22B)	111(2)
H(8A)-C(8)-H(8B)	107(3)	N(2)-C(22)-H(22B)	102(2)
N(2)-C(9)-C(6)	113.0(3)	H(22A)-C(22)-H(22B)	109(3)
N(2)-C(9)-H(9A)	110(2)	N(5)-C(23)-C(24)	121.6(4)
C(6)-C(9)-H(9A)	109(2)	N(5)-C(23)-C(22)	115.3(3)
N(2)-C(9)-H(9B)	104(2)	C(24)-C(23)-C(22)	123.1(3)
C(6)-C(9)-H(9B)	108(2)	C(25)-C(24)-C(23)	119.6(4)
H(9A)-C(9)-H(9B)	112(3)	C(25)-C(24)-H(24)	126(3)
N(1)-C(10)-C(11)	112.9(3)	C(23)-C(24)-H(24)	114(3)
N(1)-C(10)-H(10A)	105(2)	C(24)-C(25)-C(26)	119.2(4)
C(11)-C(10)-H(10A)	101(2)	C(24)-C(25)-H(25)	122(3)
N(1)-C(10)-H(10B)	109(2)	C(26)-C(25)-H(25)	119(3)
C(11)-C(10)-H(10B)	116(3)	C(25)-C(26)-C(27)	118.9(4)
H(10A)-C(10)-H(10B)	112(3)	C(25)-C(26)-H(26)	130(3)
N(3)-C(11)-C(12)	121.1(4)	C(27)-C(26)-H(26)	111(3)
N(3)-C(11)-C(10)	115.9(3)	N(5)-C(27)-C(26)	122.4(4)
C(12)-C(11)-C(10)	122.9(4)	N(5)-C(27)-H(27)	120(2)
C(13)-C(12)-C(11)	119.4(4)	C(26)-C(27)-H(27)	118(2)
C(13)-C(12)-H(12)	121(3)	N(2)-C(28)-C(29)	110.2(3)
C(11)-C(12)-H(12)	120(3)	N(2)-C(28)-H(28A)	107(2)
C(12)-C(13)-C(14)	120.1(4)	C(29)-C(28)-H(28A)	110(2)
C(12)-C(13)-H(13)	120(3)	N(2)-C(28)-H(28B)	110(2)
C(14)-C(13)-H(13)	119(3)	C(29)-C(28)-H(28B)	114(2)
C(15)-C(14)-C(13)	117.5(5)	H(28A)-C(28)-H(28B)	105(3)
C(15)-C(14)-H(14)	124(3)	N(6)-C(29)-C(30)	121.4(3)
C(13)-C(14)-H(14)	118(2)	N(6)-C(29)-C(28)	114.5(3)
N(3)-C(15)-C(14)	123.2(4)	C(30)-C(29)-C(28)	124.1(3)
N(3)-C(15)-H(15)	116(2)	C(29)-C(30)-C(31)	119.3(4)
C(14)-C(15)-H(15)	121(2)	C(29)-C(30)-H(30)	114(2)
N(1)-C(16)-C(17)	109.7(3)	C(31)-C(30)-H(30)	127(2)
N(1)-C(16)-H(16A)	113(2)	C(32)-C(31)-C(30)	118.9(4)
C(17)-C(16)-H(16A)	107(2)	C(32)-C(31)-H(31)	117(2)
N(1)-C(16)-H(16B)	111(2)	C(30)-C(31)-H(31)	124(2)
C(17)-C(16)-H(16B)	110.4(19)	C(33)-C(32)-C(31)	119.3(4)
H(16A)-C(16)-H(16B)	106(3)	C(33)-C(32)-H(32)	119(3)
N(4)-C(17)-C(18)	121.4(3)	C(31)-C(32)-H(32)	121(3)
N(4)-C(17)-C(16)	114.8(3)	N(6)-C(33)-C(32)	122.3(4)
C(18)-C(17)-C(16)	123.8(3)	N(6)-C(33)-H(33)	114(2)
C(19)-C(18)-C(17)	119.1(4)	C(32)-C(33)-H(33)	124(2)
C(19)-C(18)-H(18)	122(2)	Cl(1)-C(41)-Cl(2)	110.5(3)
C(17)-C(18)-H(18)	118(2)	Cl(1)-C(41)-H(41A)	102(2)
C(20)-C(19)-C(18)	118.8(4)	Cl(2)-C(41)-H(41A)	111(2)
C(20)-C(19)-H(19)	124(2)	Cl(1)-C(41)-H(41B)	107(3)
C(18)-C(19)-H(19)	117(2)	Cl(2)-C(41)-H(41B)	103(3)
C(19)-C(20)-C(21)	119.5(4)	H(41A)-C(41)-H(41B)	123(3)
C(19)-C(20)-H(20)	128(3)	Cl(4)-C(42)-Cl(3)	118.3(6)
C(21)-C(20)-H(20)	112(3)	Cl(4)-C(42)-Cl(3B)	91.4(7)
N(4)-C(21)-C(20)	121.7(4)	Cl(3)-C(42)-Cl(3B)	27.6(5)

Cl(4)-C(42)-Cl(4B)	14.5(7)	O(3S2)-S(2)-O(2S2)	116.8(2)
Cl(3)-C(42)-Cl(4B)	132.4(7)	O(3S2)-S(2)-O(1S2)	114.9(2)
Cl(3B)-C(42)-Cl(4B)	105.9(4)	O(2S2)-S(2)-O(1S2)	112.2(2)
Cl(4)-C(42)-H(42A)	107.7	O(3S2)-S(2)-C(2S)	105.0(2)
Cl(3)-C(42)-H(42A)	107.7	O(2S2)-S(2)-C(2S)	103.7(2)
Cl(3B)-C(42)-H(42A)	113.9	O(1S2)-S(2)-C(2S)	102.1(3)
Cl(4B)-C(42)-H(42A)	102.1	F(1S2)-C(2S)-F(2S2)	109.1(6)
Cl(4)-C(42)-H(42B)	107.7	F(1S2)-C(2S)-F(3S2)	106.7(5)
Cl(3)-C(42)-H(42B)	107.7	F(2S2)-C(2S)-F(3S2)	103.1(5)
Cl(3B)-C(42)-H(42B)	126.3	F(1S2)-C(2S)-S(2)	114.6(4)
Cl(4B)-C(42)-H(42B)	97.5	F(2S2)-C(2S)-S(2)	113.5(4)
H(42A)-C(42)-H(42B)	107.1	F(3S2)-C(2S)-S(2)	108.8(5)
Cl(5)-C(43A)-Cl(6)	117.3(10)	O(3S3)-S(3)-O(1S3)	112.9(4)
Cl(5)-C(43A)-H(43A)	108.0	O(3S3)-S(3)-O(2S3)	118.0(3)
Cl(6)-C(43A)-H(43A)	108.0	O(1S3)-S(3)-O(2S3)	112.4(2)
Cl(5)-C(43A)-H(43B)	108.0	O(3S3)-S(3)-C(3S)	104.6(3)
Cl(6)-C(43A)-H(43B)	108.0	O(1S3)-S(3)-C(3S)	101.3(3)
H(43A)-C(43A)-H(43B)	107.2	O(2S3)-S(3)-C(3S)	105.6(2)
Cl(5B)-C(43B)-Cl(6B)	112.2(6)	F(1S3)-C(3S)-F(2S3)	113.9(5)
Cl(5B)-C(43B)-H(43C)	109.2	F(1S3)-C(3S)-F(3S3)	102.6(5)
Cl(6B)-C(43B)-H(43C)	109.2	F(2S3)-C(3S)-F(3S3)	105.2(4)
Cl(5B)-C(43B)-H(43D)	109.2	F(1S3)-C(3S)-S(3)	112.0(4)
Cl(6B)-C(43B)-H(43D)	109.2	F(2S3)-C(3S)-S(3)	113.0(3)
H(43C)-C(43B)-H(43D)	107.9	F(3S3)-C(3S)-S(3)	109.4(4)
H(1O2)-O(2)-H(2O2)	100(4)		

References.

[1] S. Torelli, M. Orio, J. Pécaut, H. Jamet, L. Le Pape, S. Ménage, *Angew. Chem. Int. Ed.* **2010**, *49*, 8249-8252.

[2] (*a*) M. Roemer, B. W. Skelton, M. J. Piggott, G. A. Koutsantonis, *Dalton Trans.* **2016**, *45*, 18817-18821; (*b*) H. Ohmori, T. Takanami, H. Shimada, M. Masui, *Chem. Pharm. Bull.* **1987**, *35*, 2558-2560; (*c*) C. L. Ford, Y. J. Park, E. M. Matson, Z. Gordon, A. R. Fout, *Science* **2016**, *354*, 741-743.

[3] (*a*) N. V. Klassen, D. Marchington, H. C. E. McGowan, *Anal. Chem.* **1994**, *66*, 2921-2925; (*b*) C. Matsubara, N. Kawamoto, K. Takamura, *Analyst* **1992**, *117*, 1781-1784.